Atmos. Chem. Phys. Discuss., 9, 26735–26776, 2009
www.atmos-chem-phys-discuss.net/9/26735/2009/

Atmospheric Chemistry and Physics Discussions

This discussion paper is/has been under review for the journal Atmospheric Chemistry and Physics (ACP). Please refer to the corresponding final paper in ACP if available.

Modeling the regional impact of ship emissions on NO_x and ozone levels over the Eastern Atlantic and Western Europe using ship plume parameterization

P. Huszar[1], D. Cariolle[2,3], R. Paoli[3], T. Halenka[1,4], M. Belda[1], H. Schlager[5], J. Miksovsky[1], and P. Pisoft[1]

[1]Department of Meteorology and Environment Protection, Faculty of Mathematics and Physics, Charles University, Prague, V Holešovičkách 2, Prague 8, 180 00, Czech Republic
[2]Centre Europeén de Recherche et de Formation Avancée en Calcul Scientifique, CERFACS/CNRS, Toulouse, France

[3]Météo-France, Toulouse, France
[4]Regular associate of the Abdus Salam ICTP, Trieste, Italy
[5]German Aerospace Center, Institute of Atmospheric Physics, Oberpfaffenhofen-Wessling, Germany

Received: 9 October 2009 – Accepted: 2 December 2009 – Published: 11 December 2009

Correspondence to: P. Huszar (peter.huszar@mff.cuni.cz)

Published by Copernicus Publications on behalf of the European Geosciences Union.

Abstract

In general, regional and global chemistry transport models apply instantaneous mixing of emissions into the model's finest resolved scale. In case of a concentrated source, this could result in erroneous calculation of the evolution of both primary and secondary chemical species. Several studies discussed this issue in connection with emissions from ships and aircrafts. In this study, we present an approach to deal with the non-linear effects during dispersion of NO_x emissions from ships. It represents an adaptation of the original approach developed for aircraft NO_x emissions, which uses an exhaust tracer to trace the amount of the emitted species in the plume and applies an effective reaction rate for the ozone production/destruction during the plume's dilution into the background air. In accordance with previous studies examining the impact of international shipping on the composition of the troposphere, we found that the contribution of ship induced surface NO_x to the total reaches 90% over remote ocean and makes 10–30% near coastal regions. Due to ship emissions, surface ozone increases by up to 4–6 ppbv making 10% contribution to the surface ozone budget. When applying the ship plume parameterization, we showed that the large scale NO_x decreases and the ship NO_x contribution is reduced by up to 20–25%. Similar decrease was found in case of O_3. The plume parameterization suppressed the ship induced ozone production by 15–30% over large areas of the focused region. To evaluate the presented parameterization, nitrogen oxide measurements over the English Channel were compared with modeled values and it was found that after activating the parameterization the model accuracy increases.

1 Introduction

Most of the time, in global and regional chemical transport models, species emitted by local sources are instantaneously mixed at the model's smallest resolved scale. In the case of chemically inert constituent, this is a reasonable simplification and the model

ACPD

9, 26735–26776, 2009

will produce accurate averaged fields. However, when considering chemically reactive species emitted by such a local source, model can generate significant discrepancy compared with the reality. This is caused by the non-linearity of the chemical processes during the dispersion of the plume released by the emission source.

The non-linear character of the processes has its origins in the high concentration disturbances at the local source, e.g. at individual exhausts of aircraft engines or ship chimneys. As in many cases chemical loss and production rates are proportional to the product of the concentrations, one can generate rapid evolution in the concentration of the species in the dispersing plume, which along with the plume itself, cannot be resolved by regional and global models. In the assessment of the contribution of certain human activity, emission type or particular species to the regional and global air pollution levels, these effects should be taken into account.

In this study, the regional and local contribution of ship emissions on the background levels of nitrogen oxides (NO_x) and on consequent ozone (O_3) production/destruction will be investigated using regional modeling framework and applying a ship plume parameterization considering NO_x emissions. As shown by Corbett (2003) ship emissions represent important economic, environmental, technological, climate and also health (Corbett and Koehler, 2007) challenges through all spatial scales. During the last 50 years, seagoing ship fuel consumption, and, consequently, the CO_2/NO_x emissions have increased significantly (Eyring et al., 2005b) and studies of impact of ship traffic on climate, atmospheric chemistry, air pollution received increased attention (Corbett, 2003; Eyring et al., 2005b).

Numerous studies have focused on the impact of ship emissions on the atmospheric chemistry, air pollution on regional (Marmer and Langmann, 2005) and global (Eyring et al., 2007; Dalsøren et al., 2009) scales but none of them considers the non-linear chemical effects concerning NO_x and O_3 evolution during ship plume dispersion. A comprehensive study involving several global models, Eyring et al. (2007), still applies instantaneous mixing into the models' grid, however, it already stresses the importance of incorporating ship plume parameterization into large scale models. Also, Davis et

al. (2001) and Kasibhatla et al. (2000) reveal significant model overestimation of NO_x against observations and attribute it to the improper treatment of the chemical evolution of ship plumes as they mix into the background atmosphere.

As a default choice, the so called "plume-in-grid" (PiG) modules could provide a solution for the above mentioned problem. These modules are available in many today's chemistry transport models (Karamchandani et al., 2002; Byun and Schere, 2006; EPRI, 2000) and are designed to treat dispersion and chemical conversion of species released from large point sources realistically. Numerous studies claimed that applying PiG approach results in different large scale concentrations modeled (Vijayaraghavan et al., 2006; Karamchandani et al., 2006; Vijayaraghavan et al., 2008). Implementing PiG for ship NO_x emissions meets however unavoidable obstacles. In case of ship engine chimneys, the number of individual emitting sources can be counted in hundreds at a time and modelling NO_x plumes from all of them individually would be computationally impossible. Another difficulty arises from the fact that these sources are moving. Therefore, a different and computationally simpler approach has to be applied in case of ship emissions.

For accounting for the subgrid scale chemical processes, Franke et al. (2008) suggested to use effective emissions. This means that the actual ship emissions are changed and emissions of secondary species (ozone) are added. Here we introduce a different and novel approach to parameterize the non-linear chemical processes within the plume and implement and apply it for ship NO_x emissions. The basic ideas of this parameterization lies in the introduction of an "exhaust or fuel tracer" that traces the fraction of emissions not yet diluted at large scale, and in the calculation of an effective reaction rate for the most significant chemical ozone destroying reactions working in the high-concentration phase. This approach has been developed by Cariolle et al. (2009) and was applied to evaluate the impact of aircraft NO_x emissions on tropospheric ozone. We discuss here the adaptation of the method to the ship case as both the dispersive properties of the atmosphere and the background atmosphere composition differ from the middle and upper tropospheric conditions found for air traffic case.

This paper consists of the description of the approach in Sect. 2, which is followed by the introduction of the modeling framework used, the implementation of the parameterization itself and the configuration of the simulations carried out (Sect. 3). The results are presented in Sect. 4 and finally, Sect. 5 discusses the results and conclusions are drawn.

2 The ship plume parameterization

The basic description of the parameterization is detailed by Cariolle et al. (2009) and will not be repeated here. We focus on its adaptation for the case of ship NO_x emissions and the resulting ozone production/destruction. Basically, this paper's description is general enough to adapt it to any type of concentrated NO_x source.

2.1 The basic formulation

The method assumes a transition period with timescale τ during which the ship exhaust plume is diluted in background atmosphere. The dilution process is represented by an exhaust tracer, which traces the amount of the material in the plume with high concentrations. If we denote the tracer mass mixing ratio as r_f, the injection rate as I, the Eulerian continuity equation for the tracer assuming exponential decay becomes

$$\frac{\partial r_f}{\partial t} = I - \frac{r_f}{\tau} + T_f, \quad (1)$$

where T_f stands for the horizontal and vertical transport of the tracer. Knowing the value of r_f, we can calculate the mixing ratio of any emitted species in the high-concentration phase as the product of r_f and its emission index EI (in g/kg). For the case of NO_x we obtain

$$r_{NO_x} = r_f \cdot a_{NO_x} \cdot EI_{NO_x}, \quad (2)$$

ACPD
9, 26735–26776, 2009

where $a_{NO_x}=10^{-3}\,M_{air}/M_{NO_x}$ with M_{air} and M_{NO_x} representing the molecular mass of air and NO_x respectively. The second (sink) term on the right side of Eq. (1) gives the flux of exhaust in the high concentration phase restored in the diluted phase. Using Eq. (2) this amount is $r_f \cdot a_s \cdot EI_s/\tau$ for a particular species s, and represents an additional source term in the continuity equation for the species s in the diluted phase. For the case of NO_x, this leads to modified continuity equation

$$\frac{\partial r_{\overline{NO_x}}}{\partial t} = \frac{r_f \cdot a_{NO_x} \cdot EI_{NO_x}}{\tau} + T_{\overline{NO_x}}, \quad (3)$$

where the "overlined" $\overline{NO_x}$ indicates the NO_x in the diluted phase, $T_{\overline{NO_x}}$ represents all the other source and sink terms controlling transport, dry/wet deposition, chemical conversion and emission, except ship NO_x emission, which appears in the first term on the right side of Eq. (3).

As detailed by Cariolle et al. (2009), in situations with injection of high NO_x concentrations the ozone producing cycles via the oxidation of hydrocarbons are less efficient, and the plume chemical system is dominated by rapid titration of O_3 by NO (phase I), followed by a slower O_3 destruction (phase II). In that situation the continuity ozone equation reads

$$\frac{\partial r_{O_3}}{\partial t} = \frac{-r_f \cdot a_{NO_x} \cdot EI_{NO_x}}{\tau} \cdot \left(\frac{\overline{NO_2}}{\overline{NO_x}}\text{-ratio} \right) \cdot \delta - K_{eff} \cdot r_f \cdot \rho \cdot a_{NO_x} \cdot EI_{NO_x} \cdot r_{O_3} . \delta + T_{O_3} . \quad (4)$$

2.2 Synthesis and numerical cases

Recalling Eqs. (1), (3) and (4), one obtains the system to be solved in CTMs to account for the non-linear effects of NO_x plume dilution:

$$\frac{\partial r_f}{\partial t} = I - \frac{r_f}{\tau} + T_f ,$$

$$\frac{\partial r_{\overline{NO_x}}}{\partial t} = \frac{r_f \cdot a_{NO_x} \cdot EI_{NO_x}}{\tau} + T_{\overline{NO_x}}, \quad (5)$$

$$\frac{\partial r_{O_3}}{\partial t} = \frac{-r_f \cdot a_{NO_x} \cdot EI_{NO_x}}{\tau} \cdot \left(\frac{\overline{NO_2}}{\overline{NO_x}}\text{-ratio} \right) \cdot \delta - K_{eff} \cdot r_f \cdot \rho \cdot a_{NO_x} \cdot EI_{NO_x} \cdot r_{O_3} \cdot \delta + T_{O_3},$$

where I and EI_{NO_x} are given by the emission set and must be consistent. The ratio of diluted NO_2 and NO_x are calculated in large scale 3-D model and is available at every computational box. Quantities τ and K_{eff} depend on the structure and the evolution of the plume.

The determination of τ and K_{eff} require an adequate model for the ship plume generation and dilution, coupled to a chemical scheme that includes the main reaction of the $O_3/NO_x/HO_x$ system. For the generation and dilution of ship plumes we refer to the simulations of Chosson et al. (2008) that has determined the lifetime τ for various conditions in the boundary layer. He used direct 3-D large eddy model simulations (LES) coupled to particle tracking with accounting for the uplift of the plume due to the high temperature of the exhausts. Based on those simulations we have adopted a mean value of 50 min for the lifetime of the plume, in the medium range of the determinations obtained for typical turbulent conditions.

To evaluate the value of K_{eff} we have adapted the box model used by Cariolle et al. (2009) to the characteristics of the atmosphere found in the marine boundary layers. As for the aircraft situation, we found that for NO_x loadings larger than about 1 ppbv, the O_3 production is mostly suppressed due to a large decrease in the HO_x radical concentrations that are rapidly transformed into HNO_3. A slow ozone decrease is diagnosed. Table 1 gives the corresponding estimations of K_{eff} obtained for different levels of NO_x. The values range 6–8$\times 10^{-19}$ molecules^{-1} s^{-1} cm^3, which corresponds to a quite slow destruction process. So, as discussed further below, the effect of the plume parameterization will primary be the suppression of the ozone production for the fraction of NO_x remaining in plume-form.

Due to the rather short plume lifetime we have not considered in this study the possible transformation of a fraction of the NO_x into HNO_3. This could be significant at night by hydrolysis of N_2O_5 on aerosols, but would require a good knowledge of the aerosol properties emitted by the ships. This aspect will be addressed in future work.

3 The models

For the evaluation of the regional effect of ship NO_x emissions, a modeling system consisting of regional climate model (RCM) and chemistry transport model (CTM) was applied. The models were coupled offline, meaning that the RCM was used first to generate meteorology fields and later these fields served as an input to drive CTM. As this study is intended to capture qualities and quantities of more general validity than usually done in a case study, longer term simulation were carried out and therefore, we chose the use of RCM instead of a numerical weather prediction (NWP) model.

3.1 The climate model

For the regional climate simulations RegCM Version 3 (Pal et al., 2007) regional climate model was used. RegCM was originally developed by Giorgi et al. (1993a,b) and has undergone a number of improvements described in Giorgi et al. (1999). The dynamical core of the RegCM is equivalent to the hydrostatic version of the meso-scale model MM4 (Anthes et al., 1987) and uses terrain following σ-levels. Surface processes are represented via the Biosphere-Atmosphere Transfer Scheme (BATS) and boundary layer physics is formulated following a non-local vertical diffusion scheme (Giorgi et al., 1993a). Resolvable scale precipitation is represented via the scheme taken from Pal et al. (2000), which includes a prognostic equation for cloud water and allows for fractional grid box cloudiness, accretion and re-evaporation of falling precipitation. Convective precipitation is represented using a mass flux convective scheme detailed by Giorgi et al. (1993b) while radiative transfer is computed using the radiation

package of the NCAR Community Climate Model, version CCM3 (Giorgi et al., 1999). This scheme describes the effect of different greenhouse gases, cloud water, cloud ice and atmospheric aerosols. Cloud radiation is calculated in terms of cloud fractional cover and cloud water content, and the fraction of cloud ice is diagnosed by the scheme as a function of temperature.

3.2 The chemistry transport model

The chemistry simulations in this study were carried out with the chemistry transport model CAMx. CAMx is an Eulerian photochemical dispersion model developed by ENVIRON Int. Corp. (http://www.camx.com). Currently, CAMx is used for air quality modeling all over the world by government agencies, academic and research institutions, and private consultants for regulatory assessments and general research. CAMx can use environmental input fields from a number of meteorological models (e.g. MM5, RAMS, CALMET) and emission inputs from many emissions processors. CAMx includes the options of two-way grid nesting, multiple gas phase chemistry mechanism options (CB-IV, CB-V, SAPRC99), evolving multisectional or static two-mode particle size treatments, wet deposition of gases and particles, plume-in-grid (PiG) module for sub-grid treatment of selected point sources, Ozone and Particulate Source Apportionment Technology, mass conservative and consistent transport numerics, parallel processing. It allows for integrated "one-atmosphere" assessments of gaseous and particulate air pollution (ozone, $PM_{2.5}$, PM_{10}, air toxics) over many scales ranging from sub-urban to continental.

CAMx simulates the emission, dispersion, chemical reaction, and removal of pollutants by dry/wet deposition in the troposphere by solving the pollutant (Eulerian) continuity equation for each chemical species on a system of nested three-dimensional grids. These processes are strongly dependent on the meteorological conditions, therefore CAMx requires meteorological input from a NWP model or RCM for successful run. In order to use meteorological output from RegCM in CAMx, a preprocessor utility was developed that converts RegCM generated fields into CAMx input format.

Fields required by CAMx and not available directly in RegCM's output are calculated using diagnostic tools. Pressure is computed using the known location of the σ-levels, the distribution of the surface pressure and the constant top model pressure. Geopotential height is obtained from the hydrostatic formula using the average temperature and humidity of each layer. The precipitation rates and the vertical profile of temperature and humidity are used to compute the cloud/rain water content and cloud optical depth and finally, the vertical diffusion coefficients are calculated following O'Brien (1970).

3.3 Model's configuration and implementation of the plume parameterization

In this part the most important aspects of the model's setting will be summarized, focusing on the chemical part of the modeling framework. The area of interest of this study is the Eastern Atlantic and the coastal areas of Western and Northern Europe, where one of the most intense vessel traffic occurs (the Marine Traffic project, www.marinetraffic.com). The arrangement of the domains (Fig. 1) follows this interest accordingly. The coarse 50 km×50 km spatial resolution domain spreads from the 30° W to the 15° E meridian covering remote regions of the Atlantic Ocean as well as intense ship corridors in Europe. The eastern edge of the coarse domain was chosen to cover most of Western Europe including the Alps, which may have strong forcing on meteorological condition and therefore, impact on transport of chemical species. The nested 10 km×10 km fine resolution domain focuses on the English Channel and coastal regions of France and was set up primarily to sensitivity analysis. Both domains have their center point at 49° N, 8° W. RegCM and CAMx are running on identical domains with the only difference that the climate model maintains its calculations on grid points while CAMx considers grid boxes and the average species' concentration within them. The number of grid points (boxes) (in x/y direction) for coarse and nested domains are 71×65 (70×64) and 133×103 (132×102), respectively. The climate model runs on 18 vertical levels reaching up to 5 hPa. CAMx carries out its calculations on the first 12 levels involving the lower and middle troposphere up to 5 km. As the time

ACPD
9, 26735–26776, 2009

frame for the simulations, year 2004 was chosen. The RCM was run with additional two months in the beginning as a spin-up to ensure enough time for balancing the atmosphere.

Initial and boundary conditions for the climate run were interpolated from the ERA40 reanalysis (Uppala et al., 2005). The chemistry runs were started from clean initial conditions. In long term simulations, photochemistry is driven mainly by emissions and weather conditions so the effect of the initial conditions is almost negligible (Eben et al., 2005). Boundary conditions are held constant and reflect typical chemical background state (Simpson et al., 2003).

UNECE/EMEP data base for the year 2003 (Vestreng et al., 2007) was used as anthropogenic emissions. These data provide annual sums of emission of NO_x, CO, non-methane volatile organic compounds (NMVOCs), SO_2, NH_3, fine particles (<2.5 µm) and coarse particles (2.5 µm to 10 µm) on a 50 km×50 km grid. Emissions are divided into eleven activity sectors. For each sector, temporal disaggregation factors taken from Winiwarter and Zueger (1996) were applied to resolve hourly emissions. These factors represent different distributions of emissions for months, days of the week and hours of the day, depending on the activity sector. Calculation of biogenic emissions for isoprene and monoterpenes follows Guenther et al. (1993). They are dependent on landuse category, foliar density, temperature at 2 m and global radiation. The chemistry scheme used in the simulations was the Carbon Bond IV (CB-IV) scheme (Morris and Myers, 1990).

The implementation of the plume parameterization (Sect. 2) into the CAMx model consisted in 1) introducing an inert tracer r_f into the model variables, 2) adding Eulerian continuity equation for this tracer (Eq. 1), 3) modifying the existing continuity equations for NO_x and O_3 by adding additional terms (Eqs. 3 and 4) and finally 4) preparation of ship emission data containing the tracer and removal of NO_x emissions from it (they are represented by the tracer emission). Practically, point 2) is done along with 1), as when adding a new species in CAMx, the model automatically builds Eulerian equation for it, so the most important step was the third one, that comprised of adding the exponential

ACPD
9, 26735–26776, 2009

decay term for the tracer, the source term for NO_x and the source/sink terms for ozone representing chemical production/destruction in phases I and II.

Emissions for ships were taken from the EMEP database which covers the region of our interest. With parameterization turned on, direct NO_x emission were not accounted for and instead, tracer's emission were introduced and matched with the emitted NO. With this choice, dimensionless emission factors EI_{NO} and EI_{NO_2} for NO and NO_2 were 1.0 and 1/9.0, respectively, with the generally accepted assumption made in Sect. 2 that 90% (10%) of the NO_x emission is composed of NO (NO_2).

Several runs for year 2004 were performed and analyzed in this study. Table 2 gives a summary of them. First, we ran the models without ship emissions describing background conditions (BC experiment). After, we performed runs with ship emissions first without using the parameterization (EXPs). In the rest of the study, with the parameterization turned on, different settings were tested to investigate the sensitivity of the results on K_{eff} and τ and the resolution (experiments starting "EXPsp_"). The results are interpreted in terms of annual and seasonal differences of species' concentration between different configurations given by Table 2 evaluated on surface or on selected vertical cross-sections.

4 Results

We first evaluate the ship induced NO_x and O_3 perturbation neglecting the plume chemistry effects. Afterwards, we investigate how the plume parameterized effects modify those perturbations.

4.1 The ship traffic's impact on NO_x and O_3 levels

The ship traffic emissions strongly modify NO_x levels not only over remote ocean but also at coastal areas and to some extent over land at greater distances from the sea. Figure 2 (upper row) shows the average difference of surface NO_x concentration be-

tween runs EXPs and BC in pptv for winter (left) and summer (right). Higher NO_x levels occur along major shipping routes enfolding Western Europe from south of the Iberian Peninsula heading north around the British Islands to Northern and Baltic Seas. Highest levels of 4–6 ppbv occur over the English Channel during both seasons with peaks up to 8 ppbv in summer. Almost everywhere along the vessel corridors, NO_x is enhanced by more than 1 ppbv. Over the distant ocean, shipping traffic enhances NO_x surface levels by hundreds of pptv. Due to transport over the land, ship emissions affect also inland concentrations. Extensive areas show NO_x increase of up to 0.5 ppbv. During the winter (summer) season, NO_x perturbation over these regions is higher (lower) due to NO_x's longer (shorter) lifetime. In relative numbers (Fig. 2, lower row), shipping contributes to total surface NO_x by up to 90% over the ocean and by 10–30% near coasts. Due to the decrease of lifetime during summer, ship NO_x over land makes negligible 1% or less, however, for winter season, slightly more, 2–4% of total surface NO_x is induced here by ships.

To see the effect of ship emissions on higher model levels, vertical cross-section along the 42.5° N latitude was analyzed. This choice represents areas of remote ocean, main shipping routes and inland as well. Figure 3 shows that due to shipping, NO_x levels are significantly perturbed only in the lowest model layers. The NO_x change propagates to higher levels over the shipping route but at the 6th model level corresponding to approximately 1300 m above the ground level (a.g.l.), it decreases to 0.05 ppbv in winter which is less then 25% of the change modeled on the surface. During the summer season, the decrease is even more rapid and the latter is modeled already at the 4th model level (~600 m a.g.l.). The relative contribution of ship NO_x to the total (Fig. 3, lower row) is significant at higher model levels, however the absolut changes are just small. Table 3 gives approximate heights of the model levels.

As it was already mentioned, during usual situations in the troposphere, increase of nitrogen oxides at moderate levels leads to production of ozone by the oxidations of hydrocarbons (Crutzen, 1974). However, during NO_x-saturated conditions, when high concentrations of NO_x occur, O_3 decreases with increasing NO_x and titration occur.

Evaluating the difference of O_3 modeled with and without ship emissions, we can detect regions of both behavior. In annual average (Fig. 4, bottom), ozone is increased over the majority of the ocean (covered by our domain) by 1–3 ppbv and ozone production occurs even over the land. However, over areas of intense ship traffic in the English Channel, Northern and Baltic Sea, ozone is destroyed by the value of 2–3 ppbv. In summer (Fig. 4, upper right), the ozone production is enhanced over the remote ocean leading to an increase of 4–6 ppbv and at the same time, ozone destruction is limited to the English Channel and smaller areas over the seas mentioned before. Ozone production over the land up to 1 ppbv also cannot be neglected. During winter, ozone formation is suppressed and takes place only over the remote sea with the magnitude up to 0.8 ppbv. In relative numbers (Fig. 5), ship induced ozone contribution to total surface ozone as annual average makes 6–8% over the remote sea, exceeding 10% over large areas during the summer period.

Going into higher model levels, Fig. 6 shows that the ship induced ozone production in annual average is exceeding 1 ppbv in the first 5 levels representing heights up to 900 m, reaching the 7th level (~1800 m) in summer.

4.2 Plume effects

In this section, we apply the knowledge learned in the Sect. 2 about the ship plume chemistry effects involving NO_x and O_3 to the evaluation of ship emission impact on atmospheric composition. Regarding NO_x, a certain fraction is remaining inside the high-concentration phase and this is expected to be invisible for the model, therefore, decrease of nitrogen dioxides should occur. Figure 7 (upper row) confirms this. With plume effects, the average surface large-scale NO_x concentration decreases by up to 0.1 ppbv over remote sea during both seasons. The reduction in the main corridors is much more intensive and exceeds 1 ppbv at peak levels in both summer and winter. This can be also interpreted as the modification of the NO_x perturbation caused by ship emissions. In relative numbers, Fig. 7 (bottom row) shows that ship NO_x perturbation is reduced by more than 10% along shipping routes. Areas of intensive ship traffic

(coastal regions and the most important shipping corridors) indicate reduction of 20–25%.

As expected in the Sect. 2, ozone production is suppressed. Figure 8 (left column) shows that ship plume effects lead to decrease of ozone in both summer and winter seasons. The reduction occurs on the whole area of the domain except negligible region in central Iberian Peninsula during summer conditions. The O_3 change is, again, largest in the shipping corridors where it reaches the values of 0.4–0.7 ppbv in winter and of 1–2 ppbv during summer conditions. As seen in previous section, the impact of shipping on ozone is not unequivocal: while at most of the remote domain, ships contribute to ozone production, regions of ozone destruction over intense shipping routes also appear. Therefore, the O_3 reduction seen in Fig. 8 will at some areas suppress the production resulted from shipping while other areas will show enhancement of O_3 destruction. We have to remember this when considering the relative change of ship induced ozone by the introduction the plume parameterization. During summer conditions and in annual average, on the majority of the domain, shipping increases ozone. In the right column of Fig. 8, the spatial distribution of the relative change of this increase accounting for plume effects is plotted (middle for summer, bottom for average annual conditions). It can be seen that O_3 production is suppressed by 15–30% over remote sea and by over 50% in and around shipping corridors. At higher model levels, the effect of plume parameterization is decreasing rapidly. Figure 9 (right) plots the O_3 decrease averaged over the whole domain. Effect of parameterization is reduced by 50% at the 3–4th model level corresponding to heights of ~600 m.

Further, the sensitivity of model results on parameters and resolution will be presented. First, the K_{eff} effective reaction rate was varied in the range of 6–8×10^{-19} molecules^{-1} s^{-1} cm^3 corresponding to experiments EXPsp_k1 and EXPsp_k2. Figure 10 indicates that the difference of surface ozone between the default experiment EXPsp and both experiments with modified K_{eff} is reaching 4–5 pptv at most during summer for EXPsp_k1 which is about 0.5% relative to the effect of parameterization with the default K_{eff}. During winter, the sensitivity on K_{eff} was even smaller and

ACPD
9, 26735–26776, 2009

is not shown here.

The dilution time τ is also a fundamental input parameter characterizing the performance of the parameterization. It directly controls the amount of the tracer in the plume and thus the amount of NO_x in the diluted and non-diluted phase through Eq. (3). Figure 11 (upper row) shows the average tracer distribution for dilution times 25 and 50 min corresponding to experiments EXPsp_t50 and EXPsp (default). Comparing the two figures, the ratio of tracer levels shows to be near 1:2, thus follows the ratio of the dilution time. Generally, we can expect near linearity between the dilution time and the average modeled tracer levels after considering the average emission rate *I* in the Eq. (1) and disregarding the transport, the r_f reaches equilibrium level as the temporal derivative on the left side of the previous equation becomes zero. According to Fig. 11 (lower row), the annual differences of surface NO_x modeled with and without parameterization for the both dilution times also follow this ratio. The response of r_f and NO_x to the change of τ influences ozone in two ways: first, following the classical chemistry pathways involving NO_x-O_3-VOCs and secondly, trough their role in the ship plume parameterization (Eq. 4). Figure 12 illustrates the annual average ozone response to ship plume effects for dilution times 25 min (left) and 50 min (right) and confirms significant sensitivity on τ.

Finally, nested runs on the 10 km spatial step domain were carried out (see Fig. 1). The emissions for the nested domain were at the same resolution (50 km×50 km) as those applied for the coarse domain meaning that we did not interpolate them into 10 km to increase emission's resolution but the original 50 km emissions were simply divided up into 10 km boxes. In this set up, the ozone reduction due to plume effects is rather the same for both resolution and season (Fig. 13).

4.3 Evaluation of ship plume parameterization using airborne measurements

It is expected, that the ship plume parameterization improves model accuracy. To confirm this, we applied the presented parameterization in model simulations of measurement campaign in June 2007 over the English Channel performed in the frame of

the EC Integrated Project QUANTIFY. Here, in situ measurements of nitrogen oxides in ship plumes and the background atmosphere were performed on board the DLR Falcon research aircraft. The NO instrument deployed uses NO/O_3 chemiluminescence technique including a zero volume upstream of the reaction chamber (Schlager et al., 1997).

During the flights the chemiluminescence detector was operated in modes for measure, zero and calibrate. The precision, accuracy and time resolution of the NO measurements were 7%, 12% and 1 s. For the simulations of the measurement flights, CAMx described in Sect. 3.2 was offline coupled with MM5 mesoscale model (Dudhia et al., 2005). The simulated nitrogen monoxide levels were confronted with those measured. The MM5-CAMx couple was run in an only slightly different configuration than the RegCM-CAMx couple, involving coarse and nested domains of spatial step 27 km and 9 km, respectively. The comparison of modeled NO levels (with and without parameterization) with the measurements is plotted in Fig. 14. The peak values in observations represent ship plumes, where the measuring aircraft was flying at low altitudes. The corresponding modeled NO levels are substantially lower for both runs with and without parameterization, but improvement is evident in the first case. It is important to emphasize that comparing the modeled levels of NO with measurements requires to evaluate the total nitrogen monoxide present in the atmosphere which is the sum of NO in the plume and the diluted large scale NO. The first can be expressed as the product of the tracer concentration and the emission factor for NO: $r_f \cdot a_{NO_x} \cdot EI_{NO}$. Thus, for the total NO we obtain:

$$NO_{total} = r_f \cdot a_{NO_x} \cdot EI_{NO} + \overline{NO} \quad (6)$$

5 Discussion and conlusions

The comparison of experiments with (EXPs) and without ship emissions (BC) confirms significant impact of shipping on atmospheric composition at the surface. The absolute

NO_x perturbation simulated follows the numbers in Eyring et al. (2007) or Kasibhatla et al. (2000). The change is higher then 0.2 ppbv over the Atlantic, exceeding 0.5 ppbv along the western coast of Europe and reaching maximum in English Channel, North Sea and the Baltic (4–6 ppbv). No significant difference occurs between winter and summer seasons. In relative numbers, findings of the latter work and e.g. by Dalsøren et al. (2009) go also in line with ours, showing that the largest contribution (80–90%) of ship NO_x emissions to total nitrogen oxides occurs over remote regions of the Atlantic, where no other sources are present. The impact near coastal zones is less due to presence of other NO_x sources from the land, but still important (10–50%).

We showed that ship nitrogen oxides perturb significantly also surface ozone. The simulated effect varies substantially between winter and summer despite the fact that ship emission's variation throughout the year is not large. The reason is in the different meteorological conditions (primarily temperature) and in the consequent photochemical processes. In summer, injection of ship NO_x into the atmosphere results in ozone formation at most of the domain reaching ozone perturbation of 4–6 ppbv over the Atlantic, making 10–15% relative contribution to total surface ozone budget. Dalsøren et al. (2009) found similar numbers for the corresponding regions. During winter, addition of nitrogen oxides results in ozone loss up to 3 ppbv, showed also in Eyring et al. (2007).

Running the simulations with the parameterization of ship NO_x emissions (simulations 4–8), the modeled surface levels of nitrogen oxides and ozone decrease significantly. It seems, that the distribution of the magnitude of the NO_x reduction due to the non-linear ship plume chemistry effects corresponds well to the distribution of ship induced NO_x meaning that the largest decrease (0.5–1 ppbv) occurs over regions with the highest ship emission impact and vice versa. However, the relative reduction (20–30%) of ship NO_x contribution is showing to be large not only along the major shipping routes, but also in those of minor significance. Reduction in ship induced O_3 enhancement also occurs. This is largest over regions, where the production is near zero, i.e. over areas of transition from ozone production and destruction (see Fig. 4),

but significant (10–30%) also elsewhere. In other words, modeling ship emission's impact applying instantaneous dilution in the model's grid cell overestimates both nitrogen oxides and ozone. This was already showed in works of Kasibhatla et al. (2000) and Davis et al. (2001) mentioned earlier. Using box model, von Glasgow et al. (2003) found even higher overestimation of about 50%. Song et al. (2003) attributes this to the shortened lifetime of NO_x inside the plume in the real case (2.5–10 times shorter than for background marine conditions), which results in lower net photochemical production of ozone.

It was already shown by previous studies that ozone production alters depending on the model's grid resolution. Those with higher resolution tend to produce less ozone than those with lower (Esler, 2003; Wild and Prather, 2006). A recent work, Charlton-Perez et al. (2009) showed, using high resolution ship plume dispersion chemical model, that ozone production increases by about 30% between the highest (200 m×200 m) and the lowest (about 1 km×1 km) model resolution. This is consistent with our findings, that the ship plume parameterization, which allows us to avoid going to high resolutions, suppresses part of the ozone production. The comparison of model results with measurements supports our approach, showing that the simulated NO levels are in better agreement with the measurements for the case when the parameterization is activated.

Two important parameters influence the results of the parameterized runs. Although our findings show low sensitivity on the effective reaction rate K_{eff}, the second parameter, dilution time τ has much more significant impact. Therefore its accurate estimation is crucial to the correct performance of the parameterization. In this study, an averaged value obtained from several simulations of ship plume dispersion representing various meteorological conditions was used. In future, it should be calculated online from the driving meteorological model to follow these variations. Another improvement could be achieved considering several phases during plume dispersion. This would require the introduction of more tracers and calculation of effective reaction rates in connection with each phase and different lifetimes for each tracer. The parameterization presented

here considers only NO_x-O_3 interactions, however other reactive species may play an important role in non-linearities during ship plume dispersion. E.g. von Glasgow et al. (2003) finds that chemical reactions on background aerosols significantly affect gas phase chemistry in the plume. In particular, nitrification is expected due to the hydrolysis of N_2O_5 on sulfate aerosols.

Regardless of these limitations, our results substantiated previous studies dealing with ship NO_x emissions and their non-linear effects on atmospheric chemistry. The parameterization introduced here appears suitable to account in global and regional CTMs for the non-linear chemistry effects during the dispersion phase of the ship NO_x emissions.

Acknowledgements. This work was supported in framework of EC FP6 Integrated project QUANTIFY, partially also under support of EC FP6 Specific targeted research project CECILIA and by the Ministry of Education of the Czech Republic (research plan MSM0021620860). Authors wish to express their thanks to DLR for measurements data, to ICTP for RegCM, NCAR for MM5, and Environ Corp. for CAMx made available as well as NCEP for boundary conditions available and EMEP for the emissions.

References

Anthes, R. A., Hsie, E. Y., and Kuo, Y. H.: Description of the Penn State/NCAR mesoscale model version 4 (MM4), Tech. Report NCAR/TN-282+STR, National Center for Atmosphere Research, Boulder, Colorado, 1987. 26743

Byun, D. and Schere, K. L.: Review of the governing equations, computational algorithms, and other components of the Models-3 Community Multiscale Air Quality (CMAQ) modeling system, Appl. Mech. Rev., 59, 51–77, 2006. 26739

Cariolle, D., Caro, D., Paoli, R., Hauglustaine, D. A., Cuenot, B., Cozic, A., and Paugam, R.: Parameterization of plume chemistry into large-scale atmospheric models: Application to aircraft NO_x emissions, J. Geophys. Res., 114, D19302, doi:10.1029/2009JD011873, 2009. 26739, 26740, 26741, 26742

Charlton-Perez, C. L., Evans, M. J., Marsham, J. H., and Esler, J. G.: The impact of resolution

on ship plume simulations with NO_x chemistry, Atmos. Chem. Phys., 9, 7505–7518, 2009, http://www.atmos-chem-phys.net/9/7505/2009/. 26754
Chosson, F., Paoli, R., and Cuenot, B.: Ship plume dispersion rates in convective boundary layers for chemistry models, Atmos. Chem. Phys., 8, 4841–4853, 2008, http://www.atmos-chem-phys.net/8/4841/2008/. 26742
Corbett, J. J. and Koehler, H. W.: Updated Emissions from Ocean Shipping, J. Geophys. Res-Atmos. 108(D20), 4650–4666, doi:10.1029/2003JD003751, 2003. 26738
Corbett, J. J., Winebrake, J. J., Green, E. H., Kasibhatla, P., Eyring, V., and Lauer, A.: Mortality from Ship Emissions: A Global Assessment, Environ. Sci. Technol., 41(24), 8512–8518, 2007.
Corbett, J. J.: New Directions: Designing Ship Emissions and Impacts Research to Inform Both Science and Policy, Atmos. Environ., 37(33), 4719–4721, 2003. 26738
Crutzen, P.: Photochemical reactions initiated by and influencing ozone in unpolluted tropospheric air, Tellus, 26, 47–57, 1974. 26748
Dalsøren, S. B., Eide, M. S., Endresen, Ø., Mjelde, A., Gravir, G., and Isaksen, I. S. A.: Update on emissions and environmental impacts from the international fleet of ships: the contribution from major ship types and ports, Atmos. Chem. Phys., 9, 2171–2194, 2009, http://www.atmos-chem-phys.net/9/2171/2009/. 26738, 26753
Davis, D. D., Grodzinsky, G., Kasibhatla, P., Crawford, J.,Chen, G., Liu, S., Bandy, A., Thornton, D., Guan, H., and Sandholm, S.: Impact of Ship Emissions on Marine Boundary Layer NO_x and SO_2 Distributions over the Pacific Basin, Geophys. Res. Let., 28(2), 235–238, 2001. 26738, 26754
Dudhia, J., Gill, D., Manning, K., Wang, W., Bruyere, C., Kelly, S., and Lackey, K.: PSU/NCAR Mesoscale Modeling System, Tutorial Class Notes and User's Guide: MM5 Modeling System Version 3, Pennsilvania State University, 2005. 26752
Eben, K., Jurus, P., Resler, J., Belda, M., Pelikan, E., Krueger, B. C., and Keder, J.: An ensemble Kalman filter for short-term forecasting of tropospheric ozone concentrations, Q. J. Roy. Meteorol. Soc., 131, 3313–3322, 2005. 26746
EPRI, SCICHEM Version 1.2: Techical Documentation. Final Report prepared by ARAP/Titan Corporation, Princeton, NJ, for EPRI, Palo Alto, CA. December 2000 (1000713), 2000. 26739
Esler, J. G.: An integrated approach to mixing sensitivities in tropospheric chemistry: A basis for the parameterization of subgrid-scale emissions for chemistry transport models, J. Geophys. Res., 108(D20), 4632, doi:10.1029/2003JD003627, 2003. 26754

Eyring, V., Köhler, H. W., van Aardenne, J., and Lauer, A.: Emissions from international shipping: 1. The last 50 years, J. Geophys. Res., 110, D17305, doi:10.1029/2004JD005619, 2005.
Eyring, V., Köhler, H. W., Lauer, A., and Lemper, B.: Emissions from international shipping: 2. Impact of future technologies on scenarios until 2050, J. Geophys. Res., 110, D17306, doi:10.1029/2004JD005620, 2005. 26738
Eyring, V., Stevenson, D. S., Lauer, A., Dentener, F. J., Butler, T., Collins, W. J., Ellingsen, K., Gauss, M., Hauglustaine, D. A., Isaksen, I. S. A., Lawrence, M. G., Richter, A., Rodriguez, J. M., Sanderson, M., Strahan, S. E., Sudo, K., Szopa, S., van Noije, T. P. C., and Wild, O.: Multi-model simulations of the impact of international shipping on Atmospheric Chemistry and Climate in 2000 and 2030, Atmos. Chem. Phys., 7, 757–780, 2007, http://www.atmos-chem-phys.net/7/757/2007/. 26738, 26753
Franke, K., Eyring, V., Sander, R., Hendricks, J., Lauer, A., and Sausen, R.:Toward Effective Emissions of Ships in Global Models, Meteorologische Zeitschrift, 17(2), 117–129(13), 2008. 26739
Giorgi, F., Marinucci, M. R., and Bates, G. T.: Development of a second generation regional climate model (RegCM2). Part I: boundary layer and radiative transfer processes, Mon. Weather Rev., 121, 2794–2813, 1993. 26743
Giorgi, F., Marinucci, M. R., Bates, G. T., and DeCanio, G.: Development of a second generation regional climate model (RegCM2). Part II: convective processes and assimilation of lateral boundary conditions, Mon. Weather Rev., 121, 2814–2832, 1993. 26743
Giorgi, F., Huang, Y., Nishizawa, K., and Fu, C.: A seasonal cycle simulation over eastern Asia and its sensitivity to radiative transfer and surface processes, J. Geophys. Res., 104, 6403–6423, 1999. 26743, 26744
von Glasow, R., Lawrence, M. G., Sander, R., and Crutzen, P. J.: Modeling the chemical effects of ship exhaust in the cloud-free marine boundary layer, Atmos. Chem. Phys., 3, 233–250, 2003, http://www.atmos-chem-phys.net/3/233/2003/. 26754, 26755
Guenther, A. B., Zimmermann, P. C., Harley, R., Monson, R. K., and Fall, R.: Isoprene and monoterpene emission rate variability: model evaluations and sensitivity analyses, J. Geophys. Res., 98, 12609–12617, 1993. 26746
Karamchandani, P., Seigneur, C., Vijayaraghavan, K., and Wu, S.-Y.: Development and application of a state-of-the-science plume-in-grid model, J. Geophys. Res., 107(D19), 4403,

doi:10.1029/2002JD002123, 2002. 26739
Karamchandani, P., Vijayaraghavan, K., Chen, S.-Y., Seigneur, C., and Edgerton, E.: Plume-in-grid modeling for particulate matter, Atmos. Environ., 40(38), 7280–7297, doi:10.1016/j.atmosenv.2006.06.033, 2006. 26739
Kasibhatla, P., Levy II, H., Moxim, W. J., Pandis, S. N., Corbett, J. J., Peterson, M. C., Honrath, R. E., Frost, G. J., Knapp, K., Parrish, D. D., and Ryerson, T. B.: Do Emissions from Ships have a Significant Impact on Concentrations of Nitrogen Oxides in the Marine Boundary Layer?, Geophys. Res. Lett., 27(15), 2229–2232, 2000. 26739, 26753, 26754
Marmer, E. and Langmann, B.: Impact of ship emissions on the Mediterranean summertime pollution and climate: A regional model study, Atmos. Environ., 39, 4659–5669, 2005. 26738
O'Brien, J. J.: A Note on the Vertical Structure of the Eddy Exchange Coefficient in the Planetary Boundary Layer, J. Atmos. Sci., 27, 1213–1215, 1970. 26745
Morris, E. R. and Myers, T. C.: User's Guide for the Urban Airshed Model. Volume I: User's Guide for the UAM (CB-IV), EPA-450/4-90-007A, US Environmental Protection Agency, 1990. 26746
Pal, J. S., Small, E. E., and Eltahir, E. A. B.: Simulation of regional-scale water and energy budgets: Representation of subgrid cloud and precipitation processes within RegCM, J. Geophys. Res., 105(D24), 29579–29594, 2000. 26743
Pal, J. S., Giorgi, F., Bi, X., Elguindi, N., Solomon, F., Gao, X., Rauscher, S. A., Francisco, R., Zakey, A., Winter, J., Ashfaq, M., Syed, F. S., Bell, J. L., Diffenbaugh, N. S., Karmacharya, J., Konare, A., Martinez, D., da Rocha, R. P., Sloan, L. C., Steiner, A. L.: Regional climate modeling for the developing world: The ICTP RegCM3 and RegCNET, B. Am. Meteorol. Soc., 88, 1395–1409, 2007. 26743
Simpson, D., Fagerli, H., Jonson, J. E., Tsyro, S., and Wind, P.: Transboundary Acidification, Eutrophication and Ground Level Ozone in Europe, PART I, Unified EMEP Model Description, EMEP Status Report, 2003. 26746
Schlager, H., Konopka, P., Schulte, P., Schumann, U., Ziereis, H., Arnold, F., Klemm, M., Hagen, D. E., Whitefield, P. D., and Ovarlez, J.: In situ observations of air traffic emission signatures in the North Atlantic flight corridor, J. Geophys. Res., 102(D9), 10739–10750, 1997. 26752
Song, C. H., Chen, G., Hanna, S. R., Crawford, J., and Davis D. D.: Dispersion and chemical evolution of ship plumes in the marine boundary layer: Investigation of O3/NOy/HOx chemistry, J. Geophys. Res., 108(D4), 4143, doi:10.1029/2002JD002216, 2003. 26754
Uppala, S. M., Kållberg, P. W., Simmons, A. J., Andrae, U., da Costa Bechtold, V., Fiorino, M.,

Gibson, J. K., Haseler, J., Hernandez, A., Kelly, G. A., Li, X., Onogi, K., Saarinen, S., Sokka, N., Allan, R. P., Andersson, E., Arpe, K., Balmaseda, M. A., Beljaars, A. C. M., van de Berg, L., Bidlot, J., Bormann, N., Caires, S., Chevallier, F., Dethof, A., Dragosavac, M., Fisher, M., Fuentes, M., Hagemann, S., Hlm, E., Hoskins, B. J., Isaksen, L., Janssen, P. A. E. M., Jenne, R., McNally, A.P., Mahfouf, J.-F., Morcrette, J.-J., Rayner, N. A., Saunders, R. W., Simon, P., Sterl, A., Trenberth, K. E., Untch, A., Vasiljevic, D., Viterbo, P., and Woollen, J.: The ERA-40 re-analysis, Q. J. Roy. Meteorol. Soc., 131, 2961–3012, doi:10.1256/qj.04.176, 2005. 26746

Vestreng, V., Mareckova, K., Kakareka, S., Malchykina, A., and Kukharchyk, T.: Inventory review 2007, Emission data reported to LRTAP Convention and NEC Directive, Stage 1 and 2review, and Review ofPM Inventories in Belarus, Republic of Moldova, Russian Federation and Ukraine, EMEP/MSC-W Technical Report 1/2007 ISSN 1504-6079, 2007. 26746

Vijayaraghavan, K., Karamchandani, P., and Seigneur, C.: Plume-in-grid modeling of summer air pollution in Central California, Atmos. Environ., 40, 5097–5109, doi:10.1016/j.atmosenv.2005.12.050, 2006. 26739

Vijayaraghavan, K., Karamchandani, P., Seigneur, C., Balmori, R., and Chen, S.-Y.: Plume-in-grid modeling of atmospheric mercury, J. Geophys. Res., 113, D24305, doi:10.1029/2008JD010580., 2008. 26739

Wild, O. and Prather, M. J.: Global tropospheric ozone modeling: Quantifying errors due to grid resolution, J. Geophys. Res., 111, D11305, doi:10.1029/2005JD006605, 2006. 26754

Winiwarter, W. and Zueger, J.: Pannonisches Ozonprojekt, Teilprojekt Emissionen. Endbericht. Report OEFZS-A-3817, Austrian Research Center, Seibersdorf, 1996. 26746

Table 1. Effective rate constants for O_3 destruction at high NO_x concentration computed for typical marine boundary level conditions.

NO_x [vmr]	K_{eff} [molecules^{-1} s^{-1} cm^3]
1.0×10^{-07}	7.0×10^{-19}
5.0×10^{-08}	7.4×10^{-19}
2.0×10^{-08}	5.5×10^{-19}

ACPD
9, 26735–26776, 2009

Table 2. Summary of runs carried out by the RegCM/CAMx off-line couple. ES stands for ship emissions, SP for ship plume parameterization, RES means the grid step in km (same in x/y direction), K_{eff} is the effective reaction rate in 10^{-19} molecules^{-1} s^{-1} cm^3 and τ denotes the dilution time in minutes.

Simulation	1	2	3	4	5	6	7	8
Simulation ID	BC	EXPs	EXPs_n	EXPsp	EXPsp_k1	EXPsp_k2	EXPsp_t50	EXPsp_n
ES	0%	100%	100%	100%	100%	100%	100%	100%
SP	OFF	OFF	OFF	ON	ON	ON	ON	ON
RES[km]	50	50	10	50	50	50	50	10
K_{eff}	–	–	–	7.0	6.0	8.0	7.0	7.0
τ[min]	–	–	–	50	50	50	25	50

Table 3. Approximate heights (above the ground level) of the top of CAMx model layers in the performed simulations in meters.

Level No.	1	2	3	4	5	6	7	8	9	10	11	12
Height [m]	80	170	340	600	960	1340	1800	2300	2900	3500	4200	5000

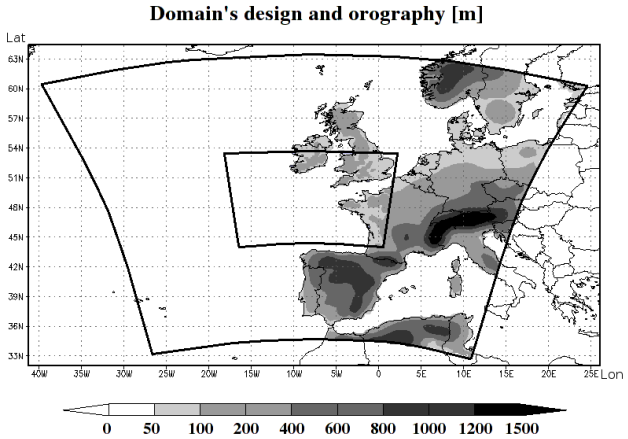

Fig. 1. RegCM/CAMx model domain's position, and orography (in meters) with the outer 50 km×50 km domain and the nested 10 km×10 km domain. (The shape of the domains is arising from the inverse projection of LCC plane to the lat-lon coordinate system.)

ACPD
9, 26735–26776, 2009

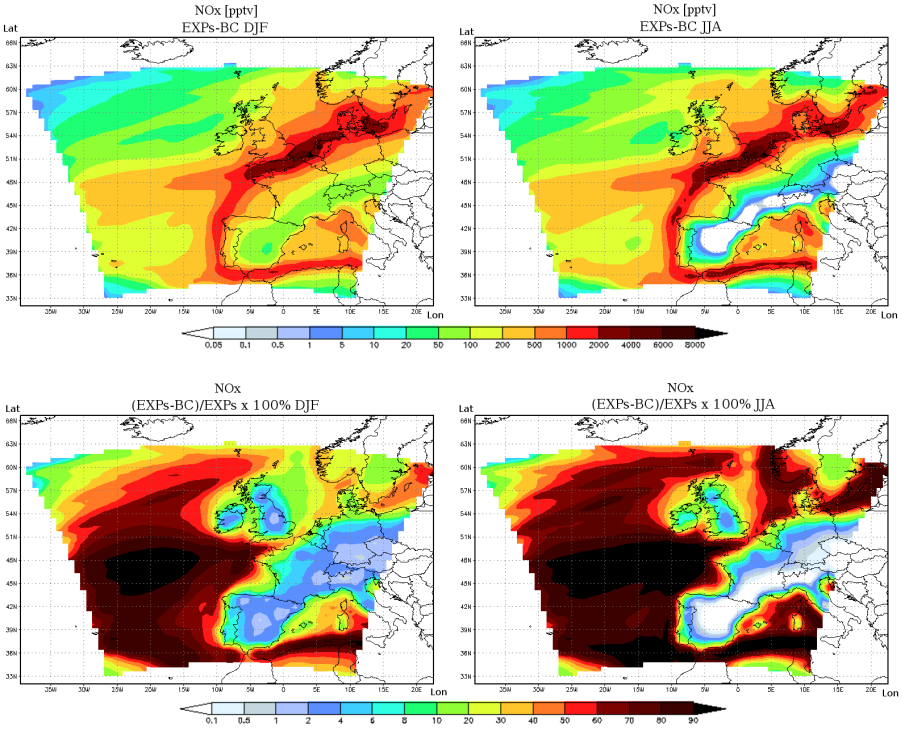

Fig. 2. The top row shows the average absolute NO_x change on surface in pptv introducing ship emissions for winter (left) and summer season (right) as difference of experiments EXPs and BC. On the bottom, the relative contribution of ship NO_x to the total NO_x as (EXPs-BC)/EXPs×100% is plotted.

ACPD
9, 26735–26776, 2009

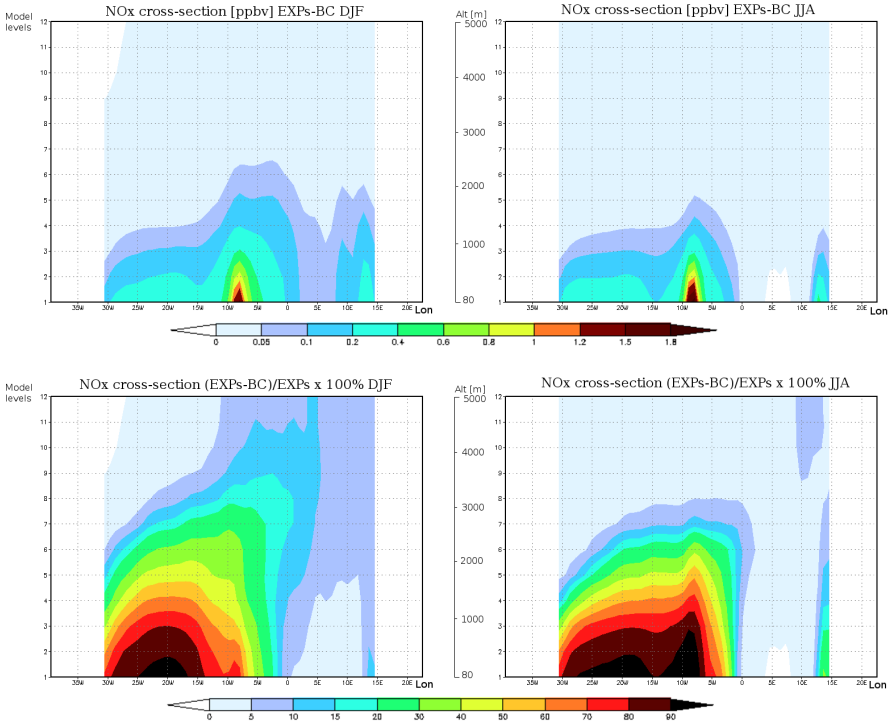

Fig. 3. Vertical cross-section along latitude 45.2° N of average absolute (top) and relative (bottom) NO_x contribution in pptv and %, respectively, to the total NO_x by introducing ship emissions for winter (left) and summer (right) season as the difference of experiments EXPs and BC with approximate altitudes.

ACPD
9, 26735–26776, 2009

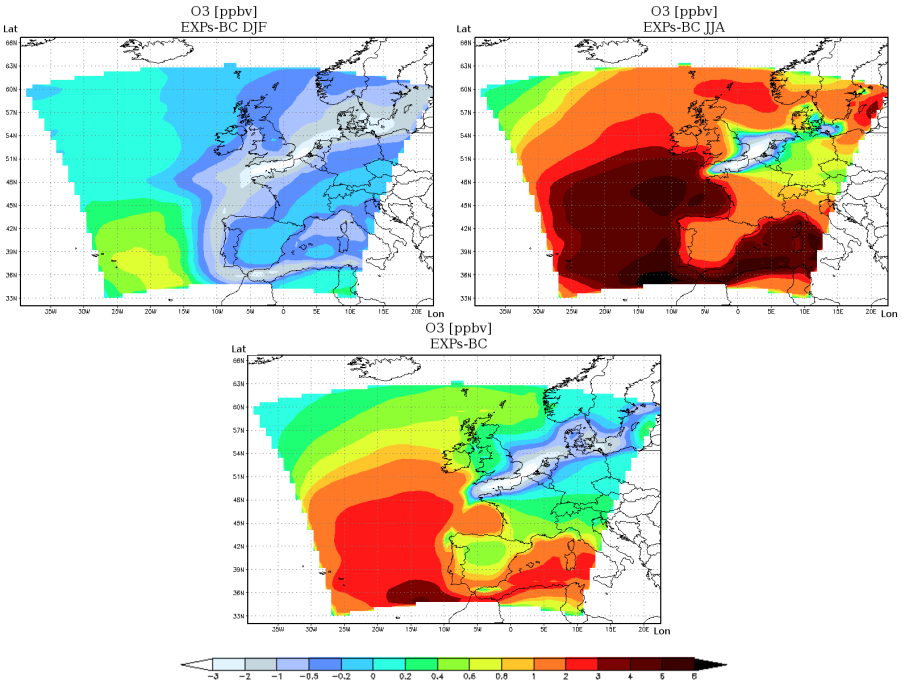

Fig. 4. Average absolute O_3 surface perturbation introducing ship emissions for winter (upper left) and summer (upper right) season and for whole year as difference of experiments EXPs and BC.

ACPD
9, 26735–26776, 2009

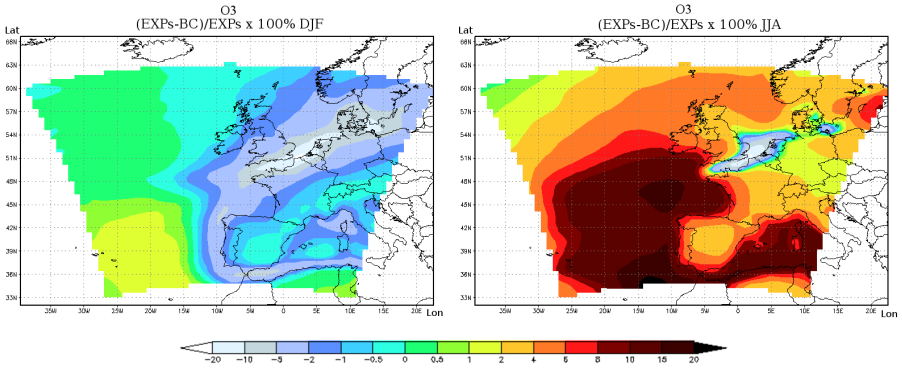

Fig. 5. Average relative contribution of ship induced O_3 to the total for winter (left) and summer (right) season as (EXPs-BC)/EXPs×100%. Negative values indicate the fraction of the destructed ozone to the total ozone simulated with ship traffic.

ACPD
9, 26735–26776, 2009

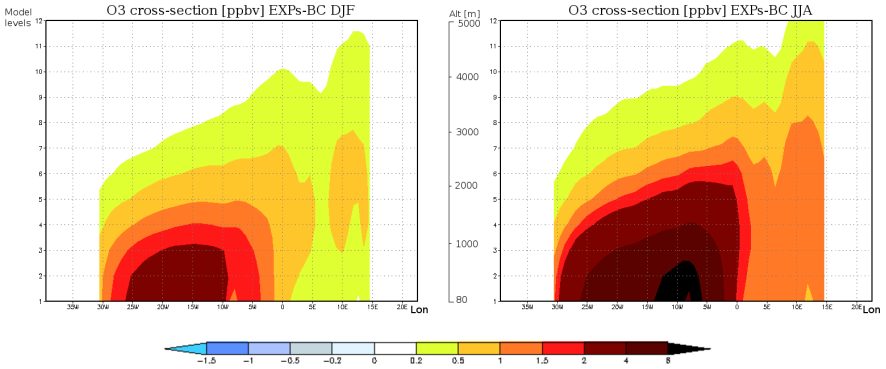

Fig. 6. Vertical cross-section along latitude 45.2° N of winter (left) and summer (right) average ship induced O_3 in ppbv as difference of experiments EXPs and BC with approximate altitudes.

ACPD
9, 26735–26776, 2009

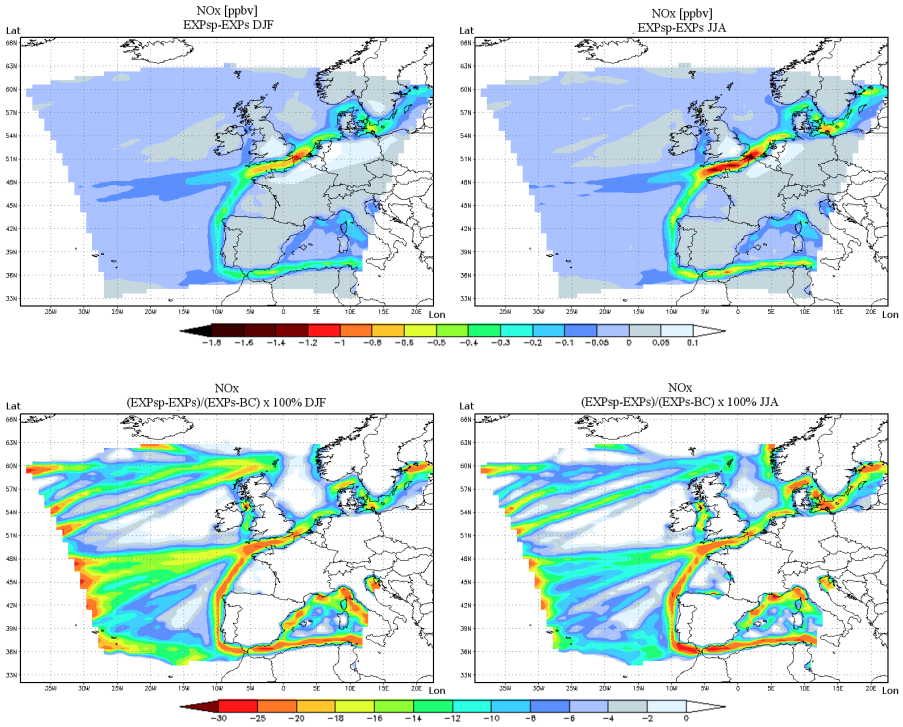

Fig. 7. Top row: difference of surface NO_x of experiments EXPsp and EXPs in ppbv for winter (left) and summer conditions (right). Bottom row: the ship induced NO_x production change as (EXPsp-EXPs)/(EXPs-BC)×100%.

ACPD
9, 26735–26776, 2009

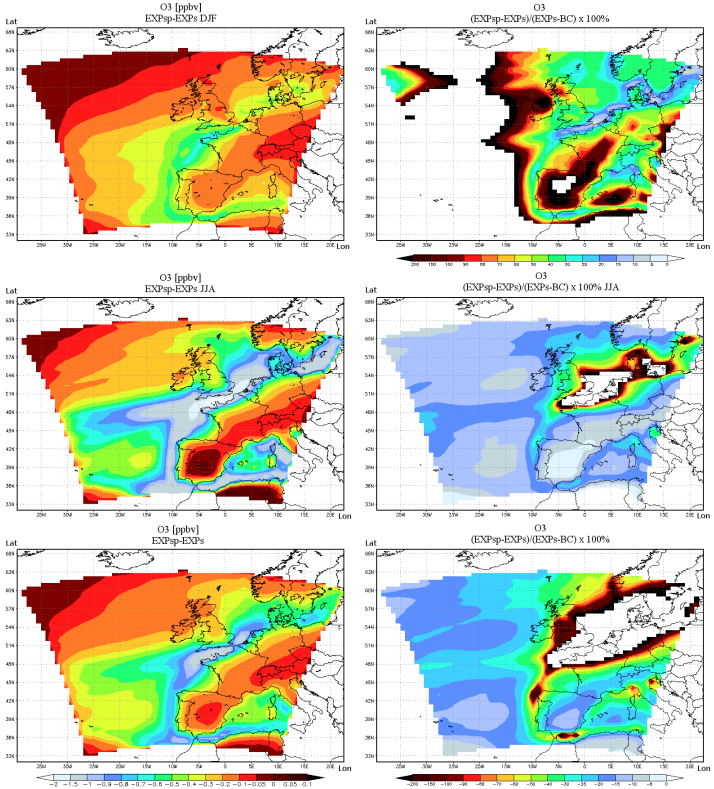

Fig. 8. Left column: difference of surface O_3 between EXPsp and EXPs in ppbv for winter (top), summer (middle) and as annual average (bottom). Right column, middle and bottom: reduction of ship ozone perturbation due to plume effects as (EXPsp-EXPs)/(EXPs-BC)×100% for summer and as annual average. Areas skipped (in white) represent regions where ship emissions cause ozone depletion. Top right figure: enhancement of ship induced O_3 destruction applying ship plume parameterization as (EXPsp-EXPs)/(EXPs-BC)×100%.

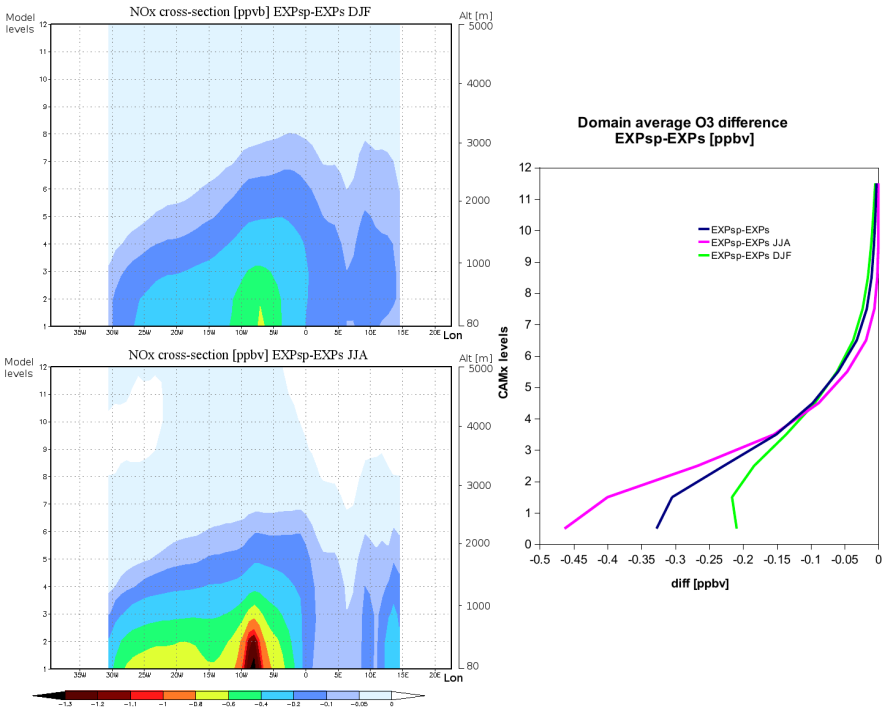

Fig. 9. Vertical cross-section along latitude 45.2° N of the difference between experiments EXPsp and EXPs for the winter (upper left) and summer season (lower left) for NO_x in ppbv with approximate altitudes. On the right: plot showing the vertical profile of the difference of EXPsp and EXPs for winter (green), summer (pink) conditions and as annual average (dark blue) for ozone averaged spatially over the entire domain.

ACPD
9, 26735–26776, 2009

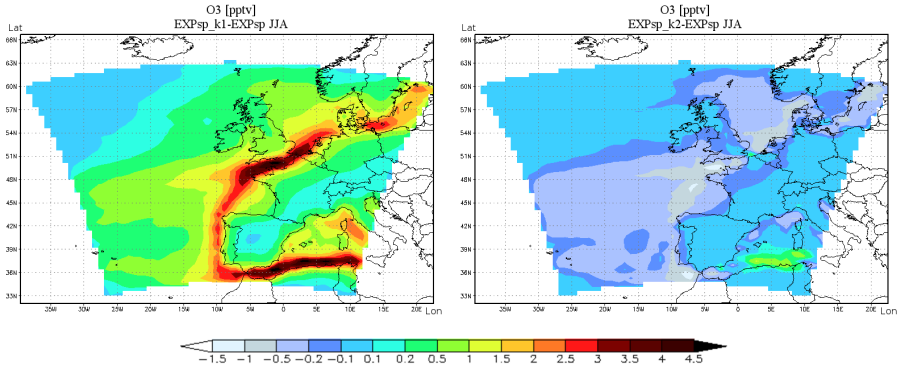

Fig. 10. Test on sensitivity on the K_{eff} parameter: difference of surface O_3 of experiments EXPsp_k1 and EXPsp (left) and EXPsp_k2 and EXPsp (right) in pptv, both for the summer season.

ACPD
9, 26735–26776, 2009

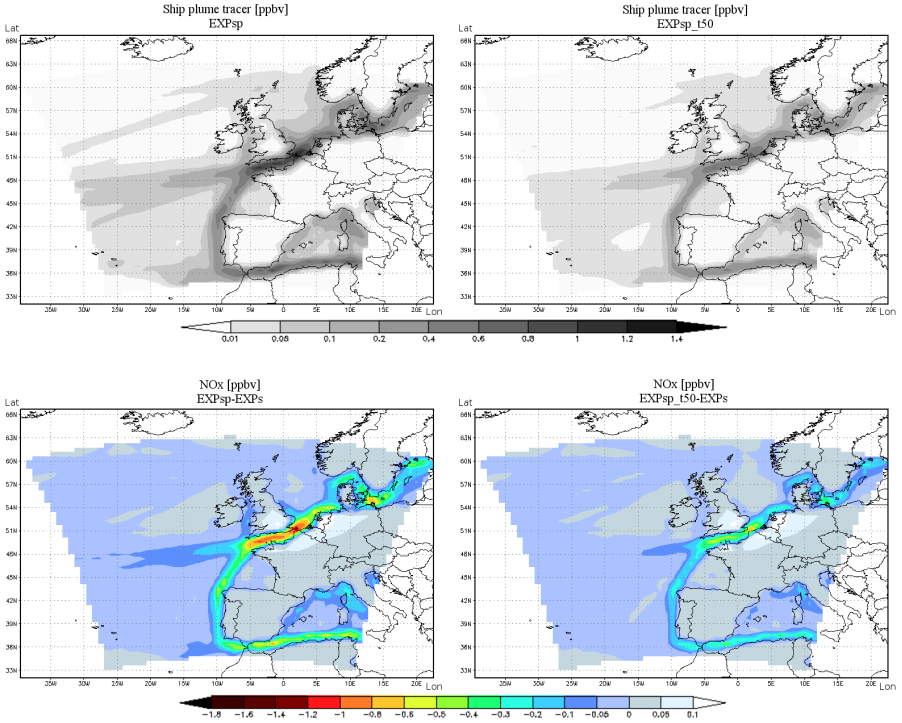

Fig. 11. Test on sensitivity on the dilution time τ. Upper row shows the tracer distribution for the default experiment EXPsp (left) and experiment EXPsp_t50 (right) with dilution time reduced by 50%. Lower panels show the surface NO_x change when applying the ship plume parameterization for "full" (left) and reduced (right) dilution time.

ACPD
9, 26735–26776, 2009

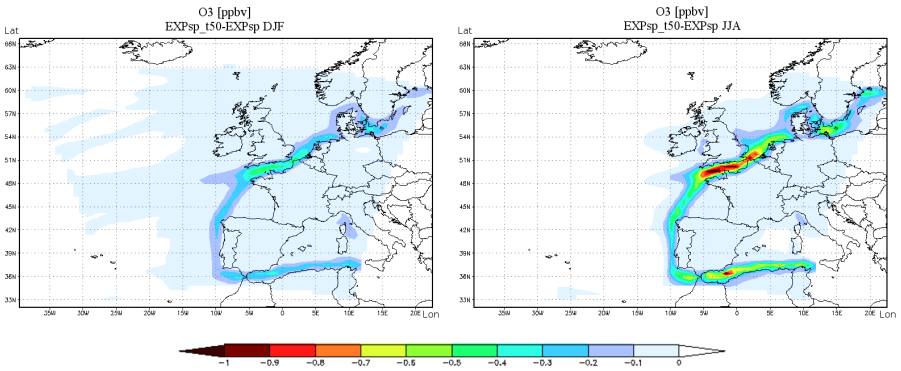

Fig. 12. Test on sensitivity on the τ parameter: surface O_3 difference between runs EXPsp_t50 and EXPsp for winter (left) and summer (right) conditions.

ACPD
9, 26735–26776, 2009

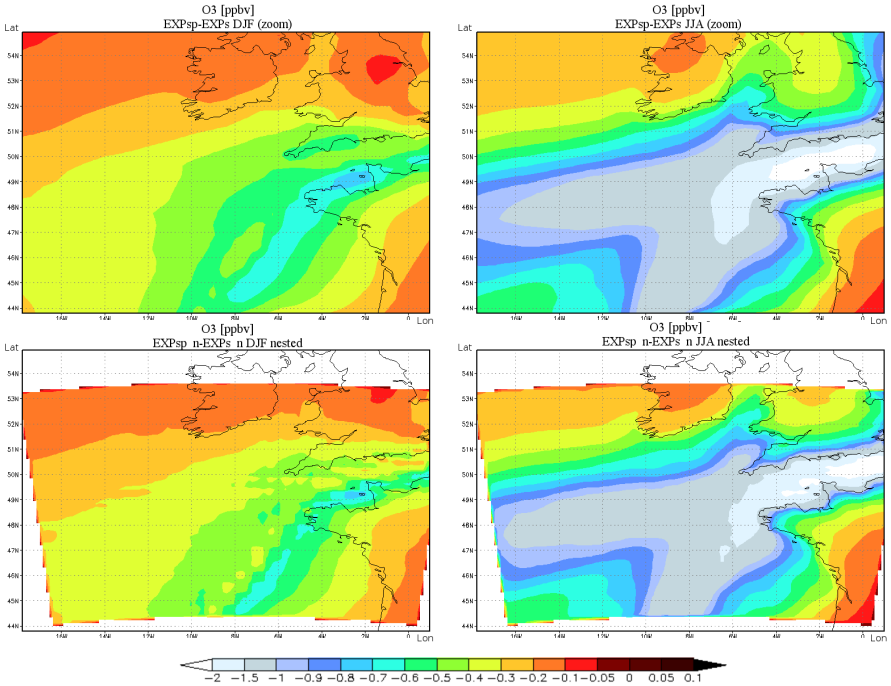

Fig. 13. Sensitivity test on the resolution. Top row: difference of surface O_3 of experiments EXPsp and EXPs zoomed on the nested 10 km domain. In the lower row: difference of EXPsp_n and EXPs_n. Concentrations are in ppbv, left column for winter, right column for summer conditions.

ACPD
9, 26735–26776, 2009

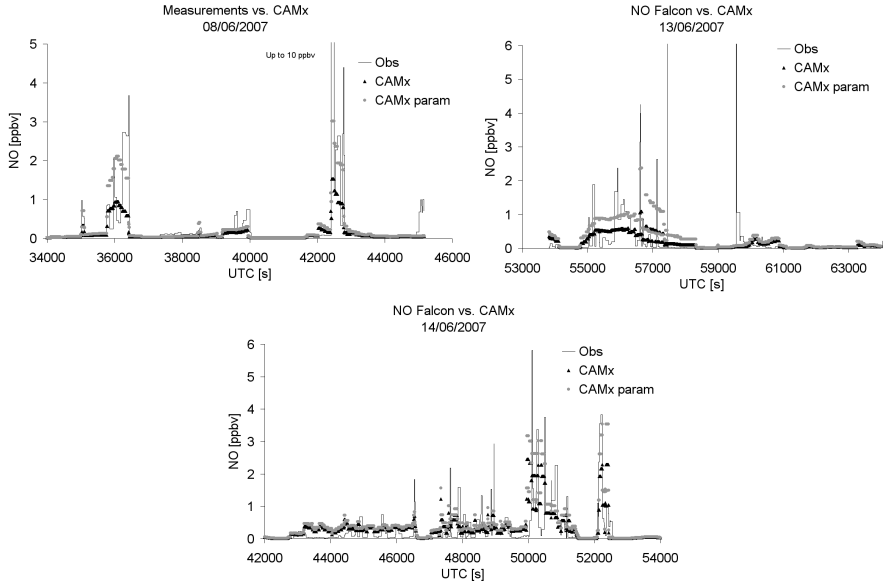

Fig. 14. Comparison of simulated nitrogen oxide levels with aircraft ship emission measurements over the English Channel in June 2007. Black triangles denote the run without the ship plume parameterization, the gray circles the run with the parameterization.